Non-Destructive Numerical Investigation of Local Heave/Liquefaction through Rock-Fill Dam upon Instrumentation Data

Seyaed Amirodin Sadrnejad
Department of Civil Engineering, K. N. Toosi University of Technology
P. O. Bax15875-4416, Tehran, Iran

Email: sadrnejad@kntu.ac.ir

Abstract

In maintenance of rock-fill dam, internal damages as any local heave or liquefaction/hydro-fracture outcome after strong earthquake shaking are detected numerically. The proposed model can rationally describe the semi-macroscopic behavior of geo-materials under the effects of any change sensed by overall instrumentation data outcome with regards to the pre-existing values before damages. The solution method is based on satisfying equilibrium, compatibility and minimum energy level as three main nature laws for any porous medium during elastic, plastic, softening, and hardening regimes. Accordingly, any compressive, tensile, shearing on plane conditions created upon experimental tests (under both quasi-static and dynamic conditions) can be numerically simulated. Any changes of displacements, stresses, strains, and even inclinations, excess pore water pressure at measuring points are converted to equivalent nodal effects and are applied to affected nodes to contribute in the solved equations. Therefore, various boundary conditions are applied to corresponding nodes creating damages or cracks as opening/ widening/closing/sliding at predefined sampling planes to change strength/permeability as the effects due to damages. The capability of proposed model in damage progression and fragmentation is investigated through the analysis of any earth structure and rock-fill dam to show the ideal damages across dam body.

Keywords: instrumentation data, shear banding, liquefaction, hydraulic fracture, damage orientation.

1. INTRODUCTION

The instrumentation of dam body and foundation plays a vital role as though any change in the structural behavior such as plastic heave, shear banding, seepage vein, etc., can be established in time based on the data observed by the instruments [1,2]. Accordingly, any remedial action and out coming measures can be taken up so as to avoid failure of the structure. Adequate instrumentation in earth fills and their foundations provide significant quantitative data indicating the magnitude and distribution of stress/strain, inclination, displacement, acceleration, pore pressures and their variations with time and other patterns of seepage, zones of potential piping, proper functioning of the filter media and effectiveness of under seepage control measures.

On the other hands, numerical analysis of the behavior of dam under any load application such as earthquake shaking and effects of existing boundary conditions, clearly, is expected to show stability through equilibrium, compatibility and under limit material behavior within continuum mechanic laws. However, any deficiency makes exceeding the limits creating abnormal differences and transferred to the location of measuring instruments. There are evidences too that exceptionally strong earthquakes have produced remarkable damages, thus showing that the actual seismic behavior of these structures is not yet fully understood, because damages are mostly internal, therefore, not directly checkable [3].

Upon an advanced model being able to present deformability orientation, failure mechanisms require applying the effects of measured quantities by instruments as equivalent nodal forces producing equal energies to abnormal difference values as mechanical load, starting with changing of stress, deformations and pore pressure at different locations in the embankments and the foundation. The limited instrument location values and impossibility of measuring continuous pressure at every point means limiting the number of measurements along certain profiles upstream and downstream from needs special cares to judge about probable damages which could occur between measuring points. Generally, pressure should be measured at any point where a variation could indicate a potential disorder. For each type of earth/rock-fill dam, design principles and modes of potential of different damage/failure are to be detailed and damage correlation to different instrument measured quantities must be investigated and clarified through the use of a capable constitutive model.

The paper concludes with the general case of dam foundation related to monitoring for any embankment dams and stresses the importance of automatic data acquisition and processing as a complement to modern dam instrumentation programs leads to the proposed damage detecting method.

2. MULTI-LAMINATE CONCEPT

For a multi-phase material such as soil that supports the overall applied loads through contact cohesion/friction, the overall mechanical response ideally may be described on the basis of micro-mechanical behaviour of grains interconnections. Naturally, this requires the description of overall stress/strain, characterization of fabric, representation of kinematics, development of local rate constitutive relations and evaluation of the overall differential constitutive relations in terms of the local quantities. Representation the overall stress/strain/compliance tensor in terms of micro level stresses and the condition, number and magnitude of contact forces has long been the aim of numerous researchers (Nemat-Nasser, et. al., (1983) [4]. The multi-laminate developed by Sadrnejad, et al., (1992, 2017) [5, 6], is capable of predicting the behaviour of geo-materials, such as rock, on the basis of sliding mechanisms, elastic behaviour of intact parts and possibilities to see different plasticity models for the most possible sliding orientations.

A multi-laminate model incorporating a mixture of the kinematic and static constraints should be physically more realistic that simply is supported by continuum mechanics law. Figure 1 shows Real aggregation of particles and 2D representation of artificial polyhedron, orientation of 17 sampling planes tangent on sphere surface and in cubes. The values of weighted coefficients of 17 independent planes are shown in Table 1.

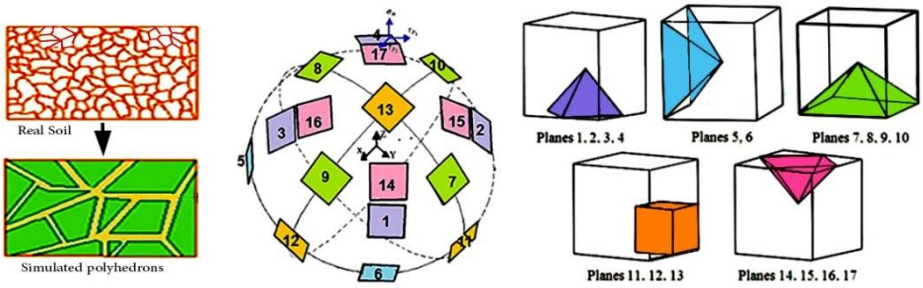

Figure 1 (a) Real aggregation of particles and simulated polyhedrons view; (b) direction of 17 sampling planes on the surface of sphere and, c) in cubes

Table 1: direction cosines and weighted coefficients for 17 planes

Plane No	normal axis			w_i
	n_1	n_2	n_3	
1	$\frac{\sqrt{3}}{3}$	$\frac{\sqrt{3}}{3}$	$\frac{\sqrt{3}}{3}$	.020277985
2	$\frac{\sqrt{3}}{3}$	$-\frac{\sqrt{3}}{3}$	$\frac{\sqrt{3}}{3}$	.020277985
3	$-\frac{\sqrt{3}}{3}$	$\frac{\sqrt{3}}{3}$	$\frac{\sqrt{3}}{3}$	.020277985
4	$-\frac{\sqrt{3}}{3}$	$-\frac{\sqrt{3}}{3}$	$\frac{\sqrt{3}}{3}$	.020277985
5	$\frac{\sqrt{2}}{2}$	$\frac{\sqrt{2}}{2}$	0	.058130468
6	$-\frac{\sqrt{2}}{2}$	$\frac{\sqrt{2}}{2}$	0	.058130468
7	$\frac{\sqrt{2}}{2}$	0	$\frac{\sqrt{2}}{2}$	.030091134
8	$-\frac{\sqrt{2}}{2}$	0	$\frac{\sqrt{2}}{2}$	.030091134
9	0	$-\frac{\sqrt{2}}{2}$	$\frac{\sqrt{2}}{2}$	.030091134
10	0	$\frac{\sqrt{2}}{2}$	$\frac{\sqrt{2}}{2}$	.030091134
11	1	0	0	.038296881
12	0	1	0	.038296881
13	0	0	1	.029390060
14	$\frac{\sqrt{6}}{6}$	$\frac{\sqrt{6}}{6}$	$\sqrt{\frac{2}{3}}$	.019070616
15	$\frac{\sqrt{6}}{6}$	$-\frac{\sqrt{6}}{6}$	$\sqrt{\frac{2}{3}}$	.019070616
16	$-\frac{\sqrt{6}}{6}$	$\frac{\sqrt{6}}{6}$	$\sqrt{\frac{2}{3}}$	.019070616
17	$-\frac{\sqrt{6}}{6}$	$-\frac{\sqrt{6}}{6}$	$\sqrt{\frac{2}{3}}$	.019070616

The created polyhedrons are roughly by 17 sliding planes, passing through each point in medium. The location of tip heads of normal to the planes defining corresponding direction cosines are shown on the surface of unit radius sphere. In ideal case, the normal integration is considered as summing up the individual micro effects correspond to infinite number of micro sampling planes. Any set of six or nine strain components apply

to *dxdydz* element sides can be transferred to a new coordinate built on a sampling plane where, one coordinate axis is normal to plane surface. According the use of 17 planes in multi-laminate numerical integration (sadrnejad, (2017)) [6], the strain tensor at any point with 6 or 9 components is equal to numerically integrated weighted 17 on plane, 3 components strain tensor. Consequentially, gradual application of abnormal differences of instrument recorded values converted to equivalent stress/strain increments and solving to satisfy minimum energy level on any of *dxdydz* element leads to carry out internal sampling plane deformations which can introduce damaged widened/slides on plane cracks. This analytical method is to be used to detect internal damages through concrete dam body. According to continuum mechanics law, any set of six or nine strain components apply to an element can be transferred to a new coordinate built on a sampling plane where, one coordinate axis is normal to plane surface. In multi-laminate frame work, the on plane micro-strain components were calculated and finally the macro-strain tensor was identified by superimposition of on-plane micro-strain components of sampling plane transformed matrix obtained through direction cosines of sampling points on the surface of a unit sphere. The basic numerical integration equation of function *f(x,y,z)*, distributed over the surface of sphere element and replacing that by strain distribution over the element surface as that function are written as follows:

$$\int_{\Omega} f(x,y,z)\,d\Omega = 4\pi \sum_{p} W_p\, f(x_p, y_p, z_p) \;\Rightarrow\; \int_{S} \varepsilon(x,y,z)\,dS = 4\pi \sum_{p} W_p\, \varepsilon(x_p, y_p, z_p) \qquad (1)$$

Furthermore, it is worth noting that to relate global stress and strain relation to this micro-level upon equation 1, it is written as follows:

$$\varepsilon_{sphere\,surface} = \int_{S} \varepsilon(x,y,z)\,dS = \int_{S} D^{-1}\sigma(x,y,z)\,dS = 4\pi \sum_{p} W_p\, D^{-1}\sigma(x_p, y_p, z_p) \qquad (2)$$

D^{-1} is material compliance matrix. According to equilibrium of forces of corresponding stresses in continuum law, the integration of stress distribution on the sphere surface is equal to the summation of on plane stresses that can be omitted from both sides of equation. Then a new integrand equation based on material compliance matrix is obtained as follows:

$$D^{-1}{}_{sphere\,surface} = \int_{S} D^{-1}(x,y,z)\,dS = 4\pi \sum_{p} W_p\, D_p^{-1}(x_p, y_p, z_p) \qquad (3)$$

Regarding the equilibrium of the forces to find three stress components on an oblique plane through element, equilibrium is satisfied. On the other hand, transferring six or nine stress components of three faces of element to new coordinate system that the oblique plane is normal to one axis of that, the same results as equilibrium will be obtained [6].

3. DAMAGE EFFECTS ON MODULUS MATRIX

In order to attain to the double constraint aspect, after analogy of the projections of stress and strain tensors on the multi-laminates, it was certain that it is possible to separate the behavior of material into two distinct parts as deviatoric and volumetric. So if we discrete the strain tensor as the volumetric and deviatoric parts firstly and then project each of them on the multi-laminates separately, we may try to obtain the deviatoric part of the modules matrix from the behaviors which are taking place on the multi-laminates and the volumetric one which is not affected by the direction characteristics and essentially is isotropic, obtained in the ordinary coordinate system and summed up to the deviatoric part at the end of each step of loading. Therefore, modulus matrix is written as follows:

$$D_{ijkl} = \frac{3}{4\pi}\int_{\Omega}\left(\frac{E}{1+\upsilon}\right)\left[\left(N_{ij} - \frac{\delta_{ij}}{3}\right)\left(N_{kl} - \frac{\delta_{kl}}{3}\right) + M_{ij}\,M_{kl} + L_{ij}\,L_{kl}\right]d\Omega + \frac{E}{1-2\upsilon}\frac{\delta_{kl}}{3}\delta_{ij} \qquad (4)$$

Total deviatoric part of constitutive matrix is computed from superposition of its counterparts in turn, are calculated based on the damage occurred on each plane depending on its specific loading conditions. This

damage is evaluated according to the five separate damage functions; each of them belongs to the particular loading states. This five loading conditions are as follows:

I. Hydrostatic Compression; II. Hydrostatic Tension; III. Pure Shear; IV. Shear + Compression; V. Shear + Tension

On each multi-laminate at each time of loading history, there exists one specific loading situation that it may be in one of the five mentioned basic loading conditions. For every five moods, a specific damage function according to the authoritative laboratory test results available in the literature is assigned. Then, for each state of on plane loading, one of the five introduced damage functions will be computed with respect to the history of micro-stress and strain components. These five damage functions are as follows:

I) hydrostatic compression: $\omega_{HC} = 0.0$ (5)

II) hydrostatic tension:

$$\omega_{HT} = 0.0 \quad if \quad \varepsilon_{eq} \le \sqrt{3}\,a$$

$$\omega_{HT} = 1.0 - \left(\frac{\sqrt{3}\,a}{\varepsilon_{eq}}\right) \times \exp\left[-\left(\frac{\varepsilon_{eq} - \sqrt{3}\,a}{b - \sqrt{3}\,a}\right)\right] \quad if \quad \varepsilon_{eq} > \sqrt{3}\,a \tag{6}$$

III) pure shear: $\omega_{SH} = 0.5 \times (\omega_C + \omega_T)$ (7)

IV) shear + compression:

$$\omega_C = d \times \varepsilon_{eq} \quad if \quad \varepsilon_{eq} \le e$$

$$\omega_C = f\left(\varepsilon_{eq} - e\right)^2 + g\left(\varepsilon_{eq} - e\right) + h \quad if \quad e < \varepsilon_{eq} \le i$$

$$\omega_C = 1.0 - \left(\frac{j}{\varepsilon_{eq}}\right) \times \exp\left[-\left(\frac{\varepsilon_{eq} - i}{k - i}\right)\right] \quad if \quad \varepsilon_{eq} > i \tag{8}$$

V) shear + tension:

$$\omega_T = 0.0 \quad if \quad \varepsilon_{eq} \le a$$

$$\omega_T = 1.0 - \left(\frac{a}{\varepsilon_{eq}}\right) \times \exp\left[-\left(\frac{\varepsilon_{eq} - a}{c - a}\right)\right] \quad if \quad \varepsilon_{eq} > a \tag{9}$$

Parameters *a* to *k* in the above relations are computed according to laboratory results obtained for each specific concrete. ε_{eq} in equations (5) to (9), is equivalent or combined average strain and in the other relations stands for the magnitude of projected deviatoric strain vector on each sampling plane. Linear elastic intact behavior of concrete adopted upon two parameters for ease as elasticity and Poisson's coefficients [7].

4. EQUIVALENT NODAL FORCES TO DISORDERS

Any excess disorder values of displacements, stresses and pore water pressures are balanced to equivalent nodal forces and apply to corresponding elements in whole structure with initial normal condition. Assuming large deformation u recorded, the equivalent nodal forces are calculated as follows:

$$\int B_{nl} D \delta\varepsilon dV = f \Rightarrow \int (B_0 + \delta B_{nl}) D (B_0 + \delta B_{nl}) \delta u dV = f \Rightarrow f_{eq} = \int (2B_0 D \delta B_{nl} + \delta B_{nl} D \delta B_{nl}) \delta u dV \tag{10}$$

Assuming excess stresses $\delta\sigma$ recorded, the equivalent nodal forces are calculated as follows:

$$\int B_{nl} \delta\sigma dV = f \Rightarrow \int (B_0 + \delta B_{nl}) \delta\sigma dV = f \Rightarrow f_{eq} = \int \delta B_{nl} \delta\sigma dV \tag{11}$$

Assuming excess pore water pressure δp recorded, the equivalent nodal forces are calculated as follows:

$$\int B_{nl} \delta p dV = f \Rightarrow \int (B_0 + \delta B_{nl}) \delta p dV = f \Rightarrow f_{eq} = \int \delta B_{nl} \delta p dV \tag{12}$$

Assuming excess strain $\delta\varepsilon$ recorded, the equivalent nodal forces are calculated as follows:

$$\int B_{nl} D \delta\varepsilon dV = f \Rightarrow \int (B_0 + \delta B_{nl}) D \delta\varepsilon dV = f \Rightarrow f_{eq} = \int \delta B_{nl} D \delta\varepsilon dV \tag{13}$$

Adding incrementally these equivalent forces and corresponding strains, damage functions approach to one and stiffness matrices start decreasing. Therefore, more volumetric strains increase with on plane normal

strains are created and permeability coefficients increase lead to less pore water pressure and more seepage flows.

5. ZIPINGPU CFRD AND WENCHUAN EARTHQUAKE

The strong ground motion (Ms = 8.0) of the 2008 Wenchuan earthquake in Sichuan Province of China caused severe damage to the Zipingpu concrete face rock-fill dam (CFRD) [1, 8, 9]. The maximum crest settlement was approximately 1.0 m, and several local failure and joint dislocations were observed in the reinforced concrete face slabs. Figure 2 shows cross section geometry and three-dimension FEM mesh of dam employed in numerical analysis. The three components of acceleration time history of earthquake and global/local damages as face slab sheared line [10, 11, 12] are shown in Figure 3-a, b, c and d, respectively. The site measuring analysis represented that the rupture process of the earthquake has extended along the fault from south to north east up to more than 300km. The represented seismic source time function displays a sequence of rupture cause a quite long duration with a total interval of about 120 s as shown in Figure 4. However, the conducted calculation showed that the only the first 16 seconds, particularly the last 6 seconds (i.e. since 10th to 16th seconds) of this time history was enough to create some on plane failure (as a set of initial damages) in face slabs at elevation 850 m.a.s.l. Exceeding the stated failure condition (till 16th second), the calculation was stopped.

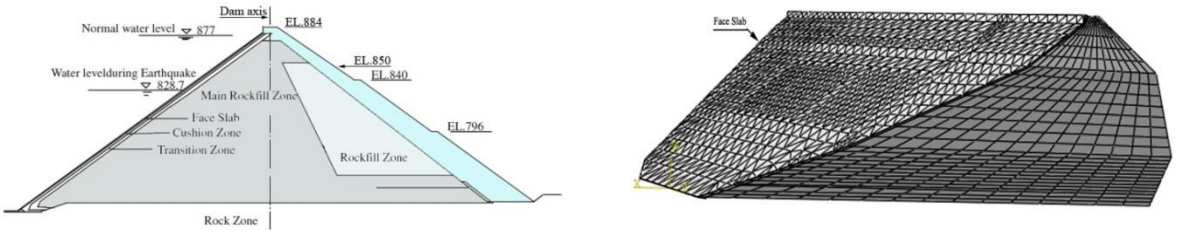

Figure 2 a) Dam cross section geometry [11], b) 3D FEM mesh

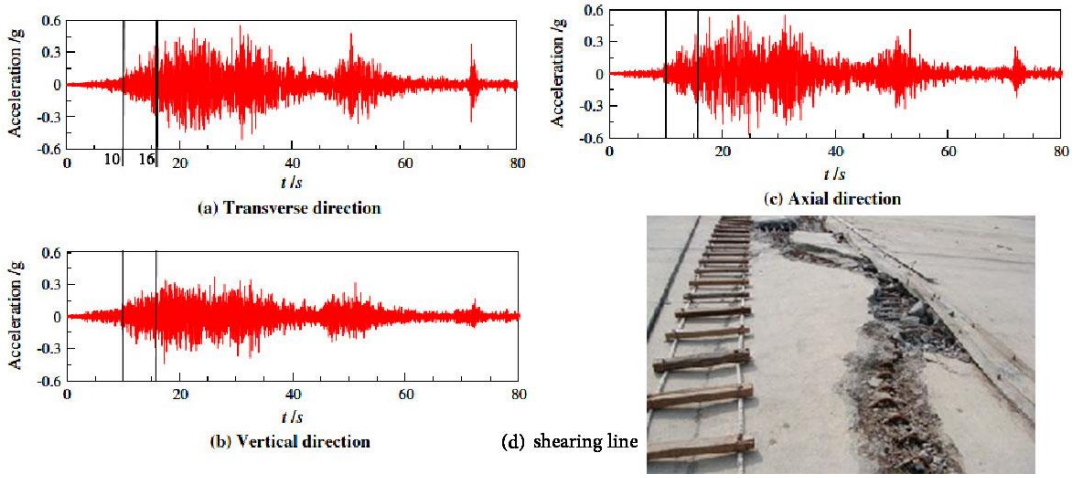

Figure 3 a, b, and c) three components of acceleration time histories, and d) global and local damages in dam concrete face [10].

The most critical point close to the selected position at elevation 850 has been supervised during the stated time period. The on plane normal and shear stress time histories of 17 planes are recorded and presented to control and compared with each other to check the priority. Figure 4-a to –c shows on plane normal stress during 6 seconds. Also, Figure 5-a to –c shows on plane shear stress during the same period. It must be noted that all 17 planes were active during earthquake shaking, however, planes number 2, 5, 6, and 11met failure showing damage coefficient equal to 1. Figure 5-d shows the orientation of failed planes. The final stress components values on plane number 5, 6, and 11reveal that there are a few shear stresses, however, tensile stress caused tensile failure. The final stress condition on plane number 2 is not tensile; however, before this stage its damage coefficient reached 1 and failed due to high shear stress in combination with tension.

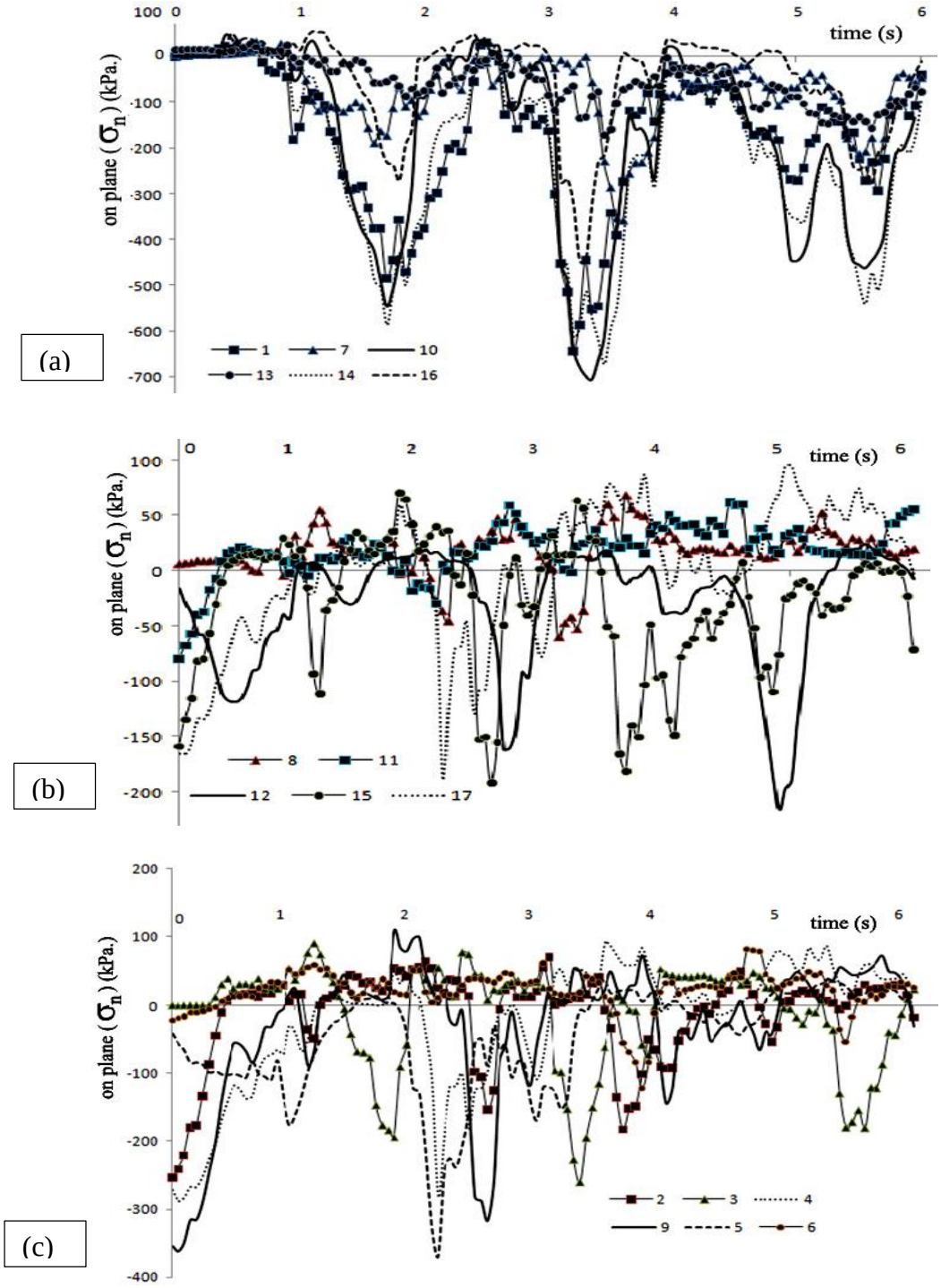

Figure 4-a to –c shows on plane normal stress during 6 seconds

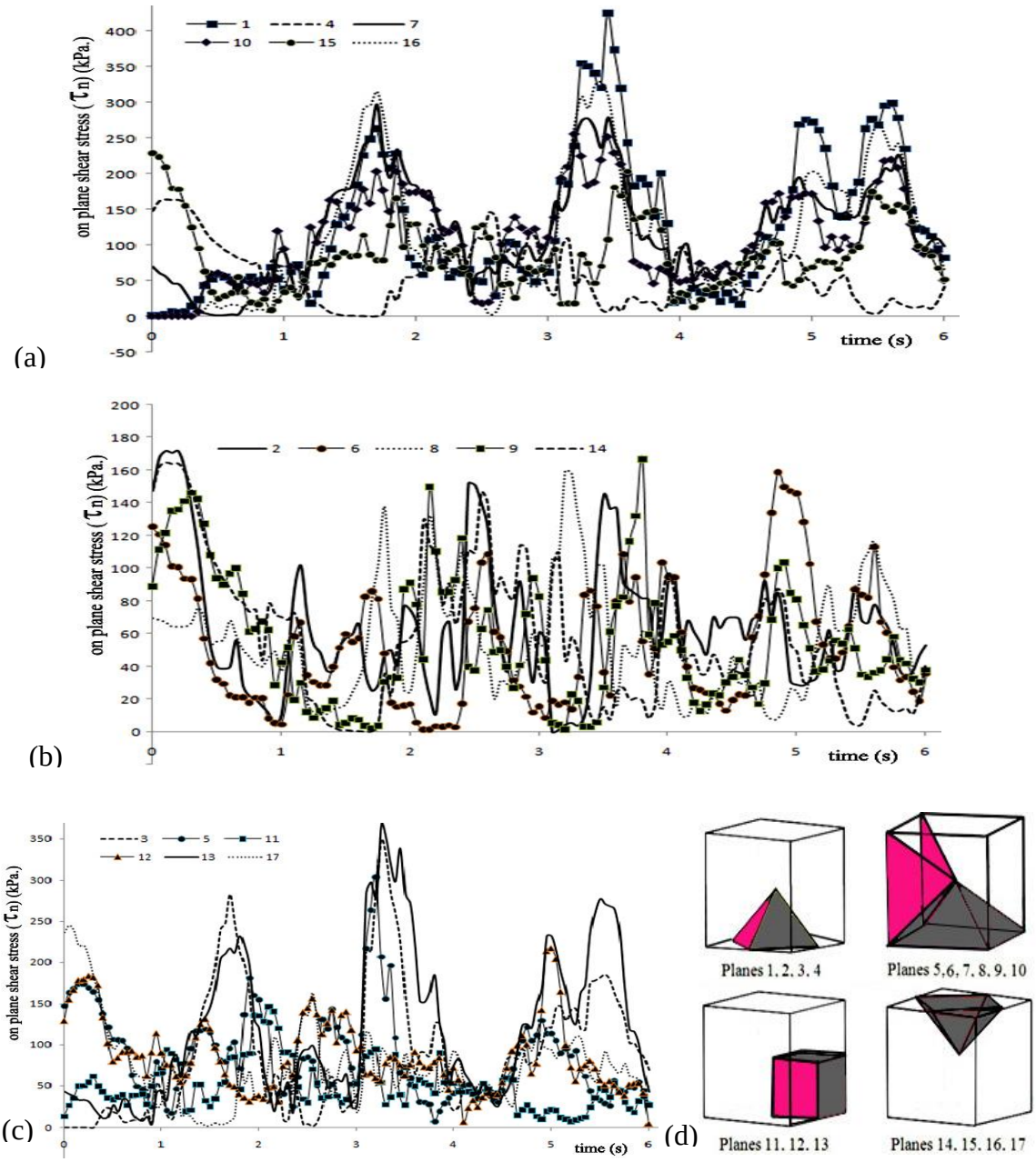

Figure 5-a to –c shows on plane shear stress during 6 seconds, d) the failed planes

To configure a continuous failure surface, a push over all failed planes in different gauss points must be plotted. However, the activity and damage progressions of gauss points located along and across sheared zone reveal a physical crushed fissured in concrete face slab and also in supporting rock fill zone shear bands. Although, only a short period of 6 seconds duration of 120 seconds earthquake time history is considered in this example, severe damaged zones including very many damaged points including several failed planes detected that show a huge crushed zone in both concrete face and supporting rock fill.

6. CONCLUSIONS

This article sets out to present the main points of how to employ instrumentation recording data to analyze numerically detecting damaged zone and types in dam static/dynamic mode. Also, it has been revealed that since each dam and its foundations represent an individual case, it is essential that a dialogue be established between the designers of the structures and the instrumentation specialists, before a site's instrumentation is determined for possibility of accurate damage detection by the proposed model.

As a result of the considerable capability of the proposed damage detecting model, the equipment recording data involved undergoes constant study designed to improve its performance and improvements can be especially notable not only in the area of improved instruments but also in automatic data acquisition and related software. Current trends in the field of instrumentation and numerical modeling emphasize the search for higher resolution and precision, providing more accurate measurements and permitting rapid detection of any behavioral anomalies. Increasing the life of these instruments as well as dam safety through strict quality control is a constant concern, moreover, with special attention paid to protection against recording accuracy due to resolution and proper location of instruments. Finally, virtually no instrumentation and corresponding location is considered complete without automatic data acquisition and processing, which increases the reliability of the results, yields more detailed analyses, with alarm thresholds, and unquestionably enhances dam safety.

In closing, it should be recalled that dam monitoring and this kind of numerical analysis is a key component of dam safety. Because the failure of a dam can lead to human as well as economic disaster, no compromise in regards to instrumentation quality or reliability should be made.

7. REFERENCES

1. Chen Houqun, (2008), CONSIDERATION OF DAM SAFETY AFTER WENCHUAN EARTHQUAKE IN CHINA, 14th World Conference on Earthquake Engineering October 12-17, 2008, Beijing, China, China Institute of Water Resources and Hydropower Research, 20, West Chegongzhuang Rd., 100044 Beijing, China
2. ICOLD Committee on Seismic Aspects of Dam Design, (2006). Reservoir Triggered Seismicity-State of knowledge, ICOLD Bulletin, Paris.
3. Chinnarasri, T. T. (2001). Numerical modelling of dam failure due to flow overtopping. Hydrological Sciences-Journal—des Sciences Hydrologiques, 46(1) February.
4. Nemat-Nasser S and Mehrabadi M. (1983) Stress and fabric in granular masses, Mechanics of granular Materials. New Models and Constitutive Relations (Eds. JT Jenkins and M. Satake), 1-8. Elsevier Sci. Pub.
5. Sadrnejad S. A., (1992) Multilaminate elastoplastic model for granular media. International Journal of Engineering 5: 11.
6. Sadrnejad S.A., Shakeri, S., (2017), Multi-laminate non-coaxial modelling of anisotropic sand behavior through damage formulation, Computers and Geotechnics 88 (2017) 18–31
7. Sadrnejad S.A. and Labibzadeh M. (2006) A continuum/discontinuum micro plane damage model for concrete. International Journal of Civil Engineering 4: 296-313.
8. Vncold. (2008). Guidelines for Design High Concrete Face Rockfill Dam.
9. Zeping, X. (2009). Performance of Zipingpu CFRD during the strong earthquake. Retrieved 05 07, 2010, from Chinese national committee of large dams: http://www.chincold.org.cn/newsview.asp?s=3226
10. Zhang, B., Wang, J., & Shi, R. (2004). Time-dependent deformation in high concrete-faced rockfill dam.
11. Wieland, M., & Houqun, C. (2009). Lessons learnt from the Wenchuan earthquake. Retrieved June 26, 2011, from: http://www.waterpowermagazine.com/graphic.asp?sc=2054099&seq=11
12. Yang, H., Haynes, M., Winzenread, S., & Okada, K. The history of dams. Retrieved May 7, 2011, from: http://cee.engr.ucdavis.edu/faculty/lund/dams/Dam_History_Page/History.htm